

https://doi.org/10.1070/QEL16431

Backward-wave spontaneous parametric down-conversion in a periodically poled KTP waveguide

I.Z. Latypov, A.A. Shukhin, D.O. Akat'ev, A.V. Shkalikov, A.A. Kalachev

Abstract. **Backward-wave spontaneous parametric down-conversion in a periodically poled potassium titanyl phosphate (KTP) crystal has been experimentally observed for the first time. The correlation and spectral characteristics of the generated single-photon states are investigated.**

Keywords: *single-photon source, spontaneous parametric down-conversion, KTP, backward-wave spontaneous parametric down-conversion.*

1. Introduction

Sources of narrow-band single- and two-photon states are important elements of devices designed for optical quantum calculations and quantum communications [1]. In particular, single-photon wave packets with a spectral width ranging from several megaherz to several gigahertz can efficiently interact with atoms and atomic ensembles and, therefore, be a basis for implementing various quantum data processing protocols using quantum memory [2]. A promising approach to the design of sources of narrow-band single-photon states is to use backward-wave spontaneous parametric down-conversion (SPDC) of light in a nonlinear waveguide [3–5]. The advantage of SPDC-based single-photon sources is that they make it possible to implement light wavelength conversion in a wide range and generate pure single-photon states at room temperature. A correlation between the signal and idler fields with respect to the number of photons allows one to herald the presence of a photon at the source output due to the detection of its partner. The contribution of multiphoton states can be reduced using single-photon detectors or applying multiplexing. An important feature of backward-wave SPDC is the narrowing of the spectrum of a photon propagating in the backward (with respect to the pump radiation) direction and suppression of the spectral correlation between the signal and idler photons, which is related to the purity of single-photon state [3, 4].

Backward-wave SPDC allows one to implement a source of single-photon states with high purity and a spectral width of ~1 GHz at room temperature. The generation efficiency can be increased by placing a nonlinear waveguide in a cavity [5]. In this configuration, the spectral width of a single-photon pulse may be reduced to a few megaherz without using additional spectral filtering and deteriorating the efficiency of conditional photon preparation. Finally, the intracavity backward-wave conversion should make it possible to generate different wave-packet shapes using pulsed laser pumping [6].

I.Z. Latypov, A.A. Shukhin, D.O. Akat'ev, A.V. Shkalikov, A.A. Kalachev Kazan E.K. Zavoisky Physical-Technical Institute, Kazan Scientific Center, Russian Academy of Sciences, ul. Sibirskii trakt 10/7, Kazan, 420029 Russia; e-mail: bibidey@mail.ru

Received 7 July 2017
Kvantovaya Elektronika **47** (9) 827–830 (2017)
Translated by Yu.P. Sin'kov

2. Main results

A periodically poled $KTiOPO_4$ waveguide (PP KTP, AdvR Inc.) was fabricated from a KTP crystal using ion implantation. The region on the crystal surface filled with rubidium atoms (Rb:KTP or RTP), which has a larger refractive index as compared with a pure KTP crystal, forms a planar waveguide. The modulation period and quality of the waveguide structure were verified in a series of experiments on second-harmonic generation at the manufacturer's laboratory. Figure 1 shows optical microscopy images of cross sections in the waveguide plane. White colour gradations correspond to the concentration of impurity Rb atoms, i.e., reflect the real waveguide structure. The refractive index profile along the z axis can be written as

$$n_j(z) = n_j^{\mathrm{KTP}} + \Delta n_j \mathrm{erfc}(-z/z_0), \quad (1)$$

where $j = Y, Z$ and $\Delta n_j = n_j^{\mathrm{RTP}} - n_j^{\mathrm{KTP}}$. The found mean depth factor z_0 turned out to be ~8.9 μm. The waveguide length was 7 mm. The effective refractive index and spatial profiles of different modes were calculated using the Comsol Multiphysics commercial software. The Sellmeier equations for $n_j^{\mathrm{KTP}}(\lambda)$ and $\Delta n_j(\lambda)$ were taken from [7] and [8], respectively. Figure 2 shows the simulation results for the fundamental modes in the KTP waveguide under study. The specific features of backward-wave SPDC in this waveguide were theoretically analysed in [9]. In particular, the generation regimes for correlated photon pairs were calculated, the spectral characteristics of the biphoton field were determined, and a comparison with the codirectional regime implemented in similar waveguides was performed.

A schematic of the experimental setup is shown in Fig. 3. The PPKTP waveguide was pumped using a 1064-nm pulsed fibre laser, consisting of a Fianium master oscillator and an ytterbium-doped fibre amplifier. The average power was 5 mW, the pulse duration was 100 ps, and the pulse repetition rate was 18 MHz. The laser pulse spectral width amounted to ~5 GHz. Parametric second-harmonic generation in a nonlinear crystal (NC) was used to obtain a pump wavelength of 532 nm.

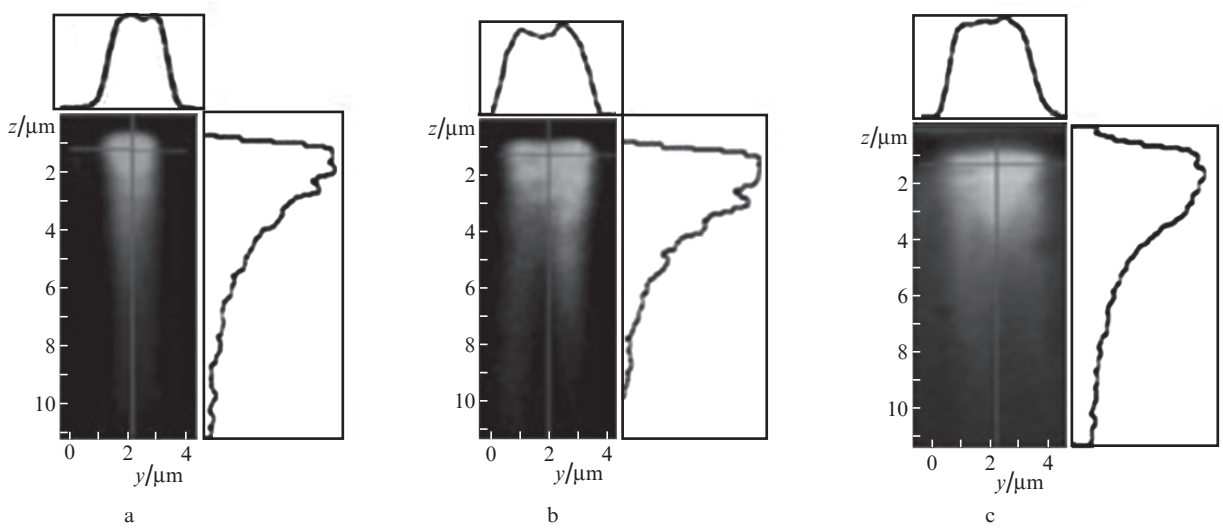

Figure 1. Optical microscopy images of waveguide cross sections. White colour grades correspond to the rubidium atom concentration (i.e., illustrate the waveguide structure). The corresponding concentration profiles are given above the images and on the right of them. The waveguide widths are (a) 2, (b) 3, and (c) 4 μm.

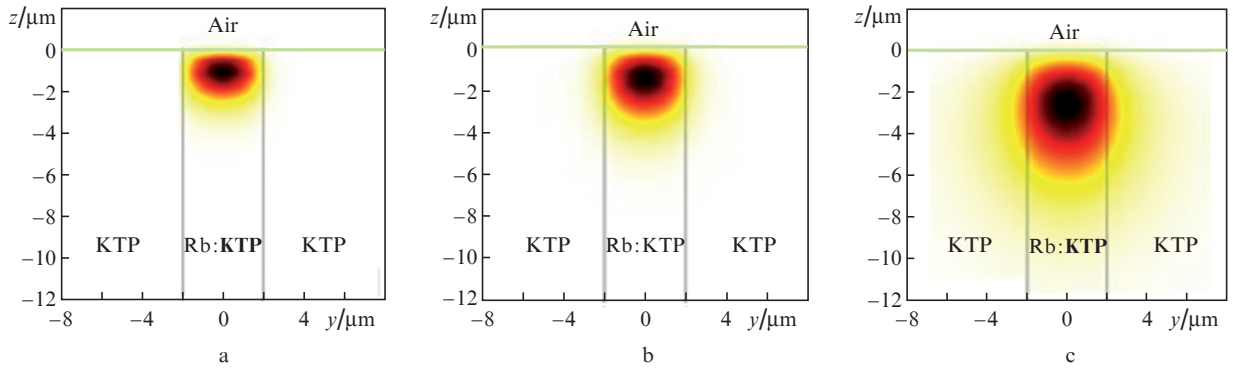

Figure 2. Intensity distributions in fundamental waveguide modes for the (a) pump radiation (λ = 532 nm), (b) signal field (λ = 810 nm), and (c) idler field (λ = 1550 nm), polarised along the Z axis ($Z \| z$). The waveguide width is 4 μm.

The pump beam was focused onto the front waveguide surface using a $10^{\times}$ optical objective (numerical aperture 0.25); the beam sizes were chosen so as to implement the most efficient excitation of the fundamental waveguide mode. The crystal was placed in a thermally stable furnace at a temperature of 32 °C, corresponding to the maximum SPDC efficiency. The signal radiation in the forward direction was collected by a $10^{\times}$ objective and transmitted through a dichroic mirror DM3 (transmission range 700–1600 nm) and a reflective diffraction grating (dispersion 3.2 nm mrad^{-1}) for fine spectral filtering. The radiation was directed (through a fibre matcher and a single-mode fibre) to an SPCM-AQRH diode avalanche photodetector, operating in the single-photon-counting regime (quantum efficiency of about 15% at a wavelength λ = 800 nm). The pump power was reduced by about 90 dB using the dichroic mirror DM3 and a diffuse scattering diffraction grating. In the opposite direction (with respect to the pump beam direction), the IR radiation passed through a mirror DM2 and was directed (using a single-mode fibre matcher) to a Scontel single-photon detector. This detector, based on superconducting nanostructures placed in a cryostat at a temperature of 2 K, has a quantum efficiency of about 30% at λ = 1550 nm; its dark count rate is ~200 Hz. The time correlations between the counts in the forward and backward channels were measured using an 8-channel time-digital ID800 converter with a time resolution of 81 ps.

The biphoton radiation, generated during backward-wave SPDC in the fifth quasi-phase-matching order, has a much lower intensity in comparison with that in the case of conventional codirectional SPDC. Therefore, a search for the SPDC signal called for a stronger suppression of the pump radiation, fluorescence signals of different kinds, and other illuminations. This problem was solved using a diffraction grating, tuned so as to make the spectral range of the radiation entering the fibre matcher aperture be equal to 4.5 nm. Tuning to the SPDC signal was performed by rotating the diffraction grating, i.e., scanning the light wavelength. The most intense (0-type) SPDC regime corresponded to signal and idler photon wavelengths of 833 and 1470 nm, respectively. All subsequent measurements were performed for this regime.

The emission spectrum of backward-wave SPDC was analysed using an SA-210 scanning Fabry–Perot resonator with a spectral resolution of 67 MHz and a dispersion range of 10 GHz (these parameters determine the spectral resolution limits) and a reflective diffraction grating with a spectral resolution of 25 GHz (with allowance for the size of the

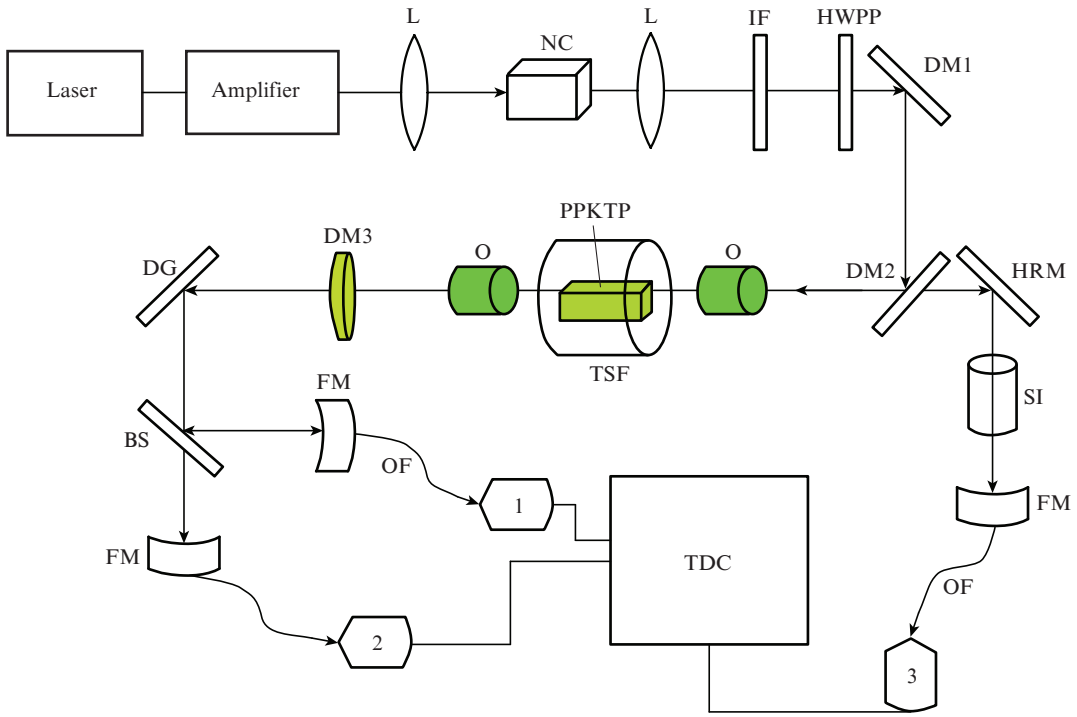

Figure 3. Schematic of the experimental setup: (L) focusing lens; (NC) nonlinear crystal for second-harmonic generation; (DM1) dichroic mirror with a transmittance of 98% at $\lambda = 1064$ nm and a reflectance of 91% at $\lambda = 532$ nm; (IF) interference filter for pump radiation at $\lambda = 532$ nm; (HWPP) half-wave phase plate for $\lambda = 532$ nm; (DM2, DM3) dichroic mirrors with a transmittance of 95% at $\lambda = 1550$ nm and a reflectance of 91% at $\lambda = 532$ nm; (O) objectives with a numerical aperture NA = 0.25; (TSF) thermally stable furnace; (DG) reflective diffraction grating with a resolution of 3.2 nm mrad^{-1}; (BS) unpolarised beam splitter; (FM) fibre matcher (aimed at introducing radiation into optical fibre); (OF) single-mode optical fibre; (1, 2) single-photon APQRH detectors; (HRM) highly reflecting mirror; (SI) scanning interferometer with a resolution of 67 MHz and a dispersion range of 12 GHz; (3) superconducting single-photon detector; (TDC) 8-channel time-digital ID800 converter with a time resolution of 81 ps.

matcher input diaphragm). The spectral width of an idler photon propagating in the backward direction was theoretically estimated to be 12 GHz for a waveguide length of 7 mm. When measuring the spectrum using a scanning Fabry–Perot cavity, we analysed the dependence of the photon count rate of detector 3 (Fig. 3) on the voltage across the cavity piezoelectric cells (the cavity mode resonance frequency is directly proportional to voltage). The presence of radiation with a spectral width of less than 10 GHz (the Fabry–Perot interferometer dispersion range) at the interferometer input would result in a peak with a magnitude significantly exceeding the broadband noise level. However, we recorded a signal corresponding to radiation with a spectral width exceeding 10 GHz. At the same time, the spectral width of an idler photon is below the width of the diffraction grating instrumental function, i.e., less than 25 GHz. Thus, we experimentally observed narrowing of the emission spectrum in the backward-wave SPDC regime in comparison with the codirectional SPDC regime by about an order of magnitude (the spectral width in the codirectional regime at the same waveguide length should to be ~250 GHz).

The correlation characteristics of generated biphoton fields were measured in the Hanbury Brown–Twiss interferometer scheme. The light beam in the signal channel was divided (using a beam splitter BS) into two beams, which were directed to detectors 1 and 2 (Fig. 3). The time marks of electric pulses from detectors 1–3 were compared on a time-digital converter, which simultaneously counted the coincidence rate on detectors 1 and 2 (R_{12}), 1 and 3 (R_{13}), and 2 and 3 (R_{23}). The rates of joint photon detection R_{13} and R_{23} are proportional to the generation rate of photon pairs, while the rate R_{12} reflects the contribution of multiphoton states. To determine exactly this contribution, one must calculate the autocorrelation function at a zero delay $g_2(0)$, which is determined by the expression [10]

$$g_2(0) = \frac{P_{12}}{P_1 P_2},\ P_{1,2} = \frac{R_{1,2}}{R_t},\ P_{12} = \frac{R_{12}}{R_t}. \qquad (2)$$

Here, $R_{1,2}$ are the count rates on detectors 1 and 2 and R_t is the photon generation rate, which is determined by dividing the count rates in each channel by total loss factors $\eta_{1,2}$ (including the loss on each optical element, the loss on the radiation input into the optical fibre, and the quantum efficiency of the detectors). The count rates on detectors 1 and 2 are related via the loss factors by a simple expression: $R_1\eta_2 = R_2\eta_1$; hence, the R_t value turns out to be the same for both channels, as one would expect. To obtain the largest number of generated photon pairs at the smallest value of the autocorrelation function $g^{(2)}(0)$, we performed an optimisation with respect to the pump power and waveguide temperature. As a result, the following values of parameters were obtained at an average pump power of 15 mW and a temperature of 32 °C: $g^{(2)}(0) = 0.012 \pm 0.004$, $R_{13} = 170 \pm 3$ pairs s^{-1}, $R_{12} = 5 \pm 1$ pairs s^{-1}, and the random coincidence rate $R_{rc} = 2 \pm 0.5$ pairs s^{-1}. The form of the autocorrelation function could not be measured under experimental conditions, because the theoretical width of the correlation function (below 200 ps) was of the same order of magnitude as the coincidence circuit resolution (80–150 ps). The photon-pair generation rate,

with allowance for the loss in the optical system, was found to be 63 kHz·mW. The efficiency of heralding the presence of a signal photon is defined as the ratio of the count rate in the idler channel to the number of count coincidences in the signal and idler channels. In our experiment, this parameter turned out to be 6% ± 0.5%.

3. Conclusions

An experiment on observing the backward-wave SPDC regime in a nonlinear periodically poled KTP waveguide was carried out. The spectral and correlation characteristics of generated single-photon states were measured. It was shown that a narrow-band source of single-photon states can be implemented based on backward-wave SPDC.

Acknowledgements. This study was supported by the Russian Science Foundation (Grant No. 14-12-00806).

References

1. Eisaman M.D., Migdall J., Fan A., Polyakov S.V. *Rev. Sci. Instrum*., **82**, 071101 (2011).
2. Sangouard N., Simon C., de Riedmatten H., Gisin N. *Rev. Mod. Phys*., **83**, 33 (2011).
3. Booth M.C., Atatüre M., Di Giuseppe G., Saleh B.E.A., Sergienko A.V., Teich M.C. *Phys. Rev. A*, **66**, 023815 (2002).
4. Christ A., Eckstein A., Mosley P.J., Silberhorn C. *Opt. Express*, **17**, 3441 (2009).
5. Chuu C.-S., Haris S.E. *Phys. Rev. A*, **83**, 061803(R) (2011).
6. Kalachev A.A. *Phys. Rev. A*, **81**, 043809 (2010).
7. König F., Wong F.N.C. *Appl. Phys. Lett*., **84**, 1644 (2004).
8. Cheng L.K., Cheng L.T., Galperin J., Hotsenpiller P.A.M., Bierlein J.D. *J. Cryst. Growth*, **137**, 107 (1994).
9. Shukhin A.A., Akatiev D.O., Latypov I.Z., Shkalikov A.V., Kalachev A.A. *J. Phys. Conf. Ser*., **613**, 012015 (2015).
10. Tengner M., Ljunggren D. arXiv:0706.2985v1.